

# Unexpected Mexiletine Responses of a Mutant Cardiac Na<sup>+</sup> Channel Implicate the Selectivity Filter as a Structural Determinant of Antiarrhythmic Drug Access

Koji Sasaki, Naomasa Makita, Akihiko Sunami, Harumizu Sakurada, Nobumasa Shirai, Hisataka Yokoi, Akinori Kimura, Noritsugu Tohse, Masayasu Hiraoka, Akira Kitabatake

*Department of Cardiovascular Medicine, Hokkaido University Graduate School of Medicine, Sapporo, Japan (K.S., N.M., N.S., H.Y., A.K.); Departments of Clinical Pharmacology (A.S.), Molecular Pathogenesis (A.Kim.), and Cardiovascular Diseases (M.H.), Medical Research Institute, Tokyo Medical and Dental University, Tokyo, Japan; Department of Cardiology, Tokyo Metropolitan Hiroo Hospital, Tokyo, Japan (H.S.); and Department of Physiology, Sapporo Medical University, Sapporo, Japan (N.T.)*

Received February 2, 2004; accepted May 20, 2004

This article is available online at <http://molpharm.aspetjournals.org>

## ABSTRACT

Gating properties of Na<sup>+</sup> channels are the critical determinants for the state-dependent block by class I antiarrhythmic drugs; however, recent site-directed mutagenesis studies have shown that the Na<sup>+</sup> channel selectivity filter region controls drug access to and dissociation from the binding site. To validate these observations, we have exploited a naturally occurring cardiac Na<sup>+</sup> channel mutation, S1710L, located next to the putative selectivity filter residue of domain 4, and evaluated the pharmacological properties to mexiletine using whole-cell, patch-clamp recordings. Consistent with the large negative shift of steady-state inactivation and the enhanced slow inactivation, the S1710L channel showed greater mexiletine tonic block than wild-type (WT) channel. In contradiction, S1710L showed attenuated use-dependent block by mexiletine and accelerated recovery from block, suggesting that the drug escape though

the external access path is facilitated. Extracellularly applied QX-314, a membrane-impermeant derivative of lidocaine, elicited significantly enhanced tonic block in S1710L similar to mexiletine. However, recovery from internally applied QX-314 was accelerated by 4.4-fold in S1710L compared with WT. These results suggest that the drug access to and dissociation from the binding site through the hydrophilic path are substantially altered. Moreover, K<sup>+</sup> permeability was 1.9-fold increased in S1710L, verifying that the mutated residue is located in the ion-conducting pore. We propose that the Na<sup>+</sup> channel selectivity filter region is a structural determinant for the antiarrhythmic drug sensitivity in addition to gating properties of the indigenous Na<sup>+</sup> channels that govern the state-dependent drug block.

Local anesthetic and class I antiarrhythmic drugs block Na<sup>+</sup> channels more potently during repetitive depolarization than during infrequent stimuli from rest. Such voltage- and frequency-dependent characteristics of Na<sup>+</sup> channel blockers are well explained by the “modulated receptor model” in which these drugs have higher affinity to inactivated Na<sup>+</sup> channels than those of closed or open states (Hille, 1977; Hondeghem and Katzung, 1977). Relevance of the gating properties of Na<sup>+</sup> channels has been also recognized in the isoform-specific difference of lidocaine sensitivity between cardiac isoform and brain/skeletal muscle isoforms. Enhanced closed-state inactivation and slow inactivation,

rather than the structural difference in the lidocaine receptor domain, mostly underlies higher lidocaine sensitivity of cardiac isoform (Nuss et al., 2000). Furthermore, investigation of a mutation of cardiac Na<sup>+</sup> channel gene *SCN5A* associated with Brugada syndrome has demonstrated that the flecainide-induced ST elevation in the patient’s electrocardiogram is attributable to the preferential interaction of flecainide with inactivated channels resulting from enhanced slow inactivation and closed-state inactivation (Viswanathan et al., 2001). These observations provide evidence that gating properties of the target Na<sup>+</sup> channels are the primary determinants for the binding of Na<sup>+</sup> channel blockers or access to the binding site, which in turn affects their clinical efficacy.

Na<sup>+</sup> channel  $\alpha$  subunits comprise four hydrophobic domains (D1–D4), each consisting of six transmembrane segments (S1–S6) (Fig. 1A). The loop connecting S5 and S6,

This study was supported by research grants 15090711 (to N.M.) from the Ministry of Education, Culture, Sports, Science and Technology, Japan, and the research grant for cardiovascular diseases (13A-1) from the Ministry of Health, Labor and Welfare, Japan, and research grant for Japan Research Foundation for Clinical Pharmacology.

**ABBREVIATIONS:** WT, wild type.

referred to as the P-loop, partially folds back into the membrane. The tips of the P-loops come together and form a narrow selectivity filter (Catterall, 2000). Two aromatic residues (Phe and Tyr) in the middle of S6 of D4 have been proposed as a part of the crucial structure required for the high-affinity binding of local anesthetic and antiarrhythmic drugs to the inactivated Na<sup>+</sup> channels (Ragsdale et al., 1994; Qu et al., 1995; Ragsdale et al., 1996). Association of Na<sup>+</sup> channel blockers with the P-loop has been recently suggested by several site-directed mutagenesis studies using membrane-impermeant lidocaine analog QX-314. QX-314 blocks cardiac Na<sup>+</sup> channels when applied from either side of the membrane but blocks neuronal Na<sup>+</sup> channels only from the intracellular side. Isoform difference of the external access path for QX-314 is localized to the cardiac-specific residues Thr near the extracellular end of D4/S6 (Qu et al., 1995) and Cys of the D1 P-loop (Sunami et al., 2000). Moreover, Sunami et al. (1997) have shown that the selectivity filter residues affect the affinity for the antiarrhythmic drugs and control their access to and dissociation from their binding site on the

cytoplasmic side of the selectivity filter. It is important to determine whether the structural alteration at the Na<sup>+</sup> channel selectivity filter region influences the actions of antiarrhythmic drugs in the clinical setting.

In the present study, we have exploited a naturally occurring *SCN5A* mutation, S1710L, associated with idiopathic ventricular fibrillation. The mutation was located at the D4 P-loop next to the residue Ala1711, one of the putative selectivity filter residues responsible for the ion permeation (Fig. 1A). Given the antiarrhythmic drug sensitivity is largely determined by the indigenous gating properties, sensitivity to the Na<sup>+</sup> channel blockers of the S1710L would be expected to be increased, because both fast and slow inactivation of the mutant channel are substantially enhanced (Akai et al., 2000; Shirai et al., 2002). Heterologously expressed mutant S1710L channel showed enhanced mexiletine tonic block, but the use-dependent block was paradoxically attenuated, probably because of structural changes at the external access paths for the antiarrhythmic drugs. We propose that the selectivity filter region per se is a structural determinant for controlling access to and dissociation from the binding site of the Na<sup>+</sup> channel blockers in addition to the indigenous gating properties.

## Materials and Methods

The S1710L mutant cDNA was constructed as human cardiac sodium channel  $\alpha$  subunit (human Na<sub>v</sub>1.5) as a template (Akai et al., 2000). Wild-type (WT) and S1710L channels were subcloned into the pRcCMV plasmid (Invitrogen). The human cell line tsA-201 was transiently transfected with WT or S1710L plasmid using the standard calcium phosphate method in combination with a plasmid encoding CD8 to visually identify transfected cells with Dynabeads M-450 CD8 (Dynal Biotech, Oslo, Norway). Na<sup>+</sup> currents were recorded 24 to 72 h after transfection using the whole-cell, patch-clamp technique as we described previously (Shirai et al., 2002). Recordings were performed at room temperature. Bath solution contained 145 mM NaCl, 4 mM KCl, 1.8 mM CaCl<sub>2</sub>, 1.0 mM MgCl<sub>2</sub>, 10 mM HEPES, pH 7.35, with NaOH, and the standard Cs<sup>+</sup>/Na<sup>+</sup> pipette solution contained 10 mM NaF, 110 mM CsF, 20 mM CsCl, 10 mM EGTA, and 10 mM HEPES, pH adjusted to 7.35 with CsOH, unless otherwise stated. In some experiments, we used a K<sup>+</sup>/Na<sup>+</sup> pipette solution containing 30 mM NaCl, 100 mM potassium aspartate, 5 mM EGTA, and 10 mM HEPES, pH adjusted to 7.2 with KOH. For experiments testing K<sup>+</sup> permeability, 145 mM NaCl in the bath solution was replaced by equimolar KCl, and the pH was adjusted to 7.35 with KOH.

Voltage-clamp command pulses were generated using pCLAMP program (Axon Instruments) and currents were filtered at 5 kHz (−3 dB; four-pole Bessel filter). Electrical resistance of the pipette was typically 1 to 2 M $\Omega$ . Voltage errors were minimized using series resistance compensation (generally 80%). Cancellation of the capacitance transients and leak subtraction were performed using an online P/4 protocol. The data were analyzed using ClampFit (Axon Instruments, Union City, CA) and SigmaPlot (SPSS Inc., Chicago, IL).

To determine the activation parameters, the current-voltage relationship was fit to the Boltzmann equation:  $I = (V - V_{\text{rev}}) \times G_{\text{max}} \times (1 + \exp((V - V_{1/2})/k))^{-1}$ , where  $I$  is the peak Na<sup>+</sup> current during the test pulse potential  $V$ . The parameters estimated by the fitting are  $V_{\text{rev}}$  (reversal potential),  $G_{\text{max}}$  (maximum conductance),  $V_{1/2}$  (voltage for half-activation), and  $k$  (slope factor). Steady-state inactivation was fit with the Boltzmann equation,  $I/I_{\text{max}} = (1 + \exp((V - V_{1/2})/k))^{-1}$  to determine the membrane potential for half-maximal inactivation ( $V_{1/2}$ ) and the slope factor  $k$ . Recovery from inactivation and

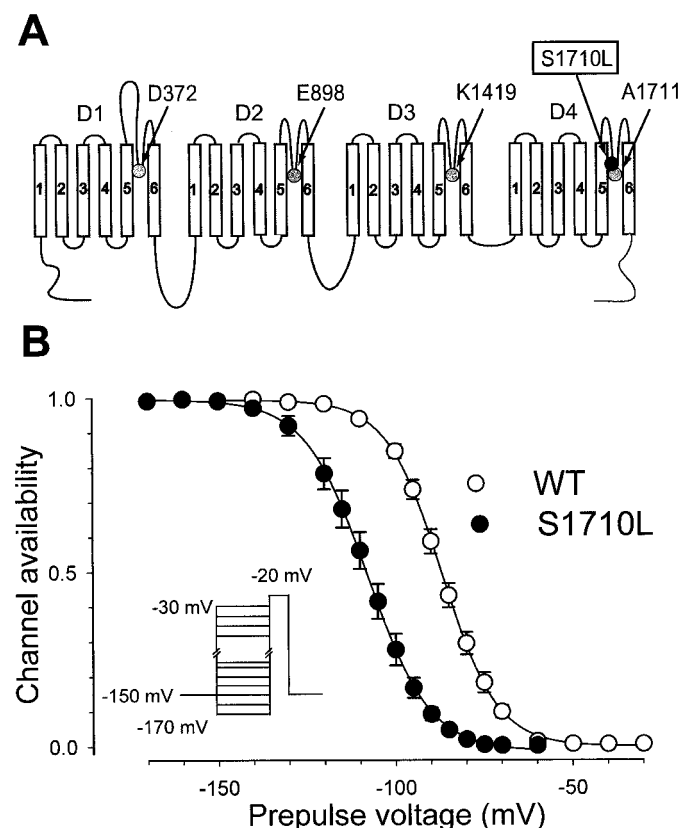


**Fig. 1.** Location of S1710L and the steady-state inactivation. A, schematic representation of the membrane topology of *SCN5A* and the location of the S1710L (●). D1–D4 indicate the homologous domains of the  $\alpha$  subunit of the cardiac Na<sup>+</sup> channel. Numbers indicate the transmembrane segments (S1–S6) of each domain. The extracellular segment between S5 and S6 of each domain, referred to as the P-loop, is proposed to fold back into the membrane and comprises a major part of the ion-conducting pore. The ion selectivity is determined by a ring of amino acids referred to as ‘DEKA’ motif (Asp372, Glu898, Lys1419, and Ala1711; ●) (Lipkind and Fozzard, 2000). B, to assess steady-state fast inactivation, the peak currents were measured during a −20 mV test potential after a series of 100-ms prepulses ranging from −170 to −30 mV from a holding potential of −150 mV. Normalized peak currents of WT (○,  $n = 6$ ) and S1710L (●,  $n = 5$ ) are plotted as a function of prepulse potential. Steady-state inactivation curve was fit with the Boltzmann equation. S1710L showed large negative shift of steady-state inactivation.

recovery from drug block were analyzed by fitting data with a double exponential equation:  $I/I_{\max} = A_{\infty} + A_f \times \exp(-t/\tau_f) + A_s \times \exp(-t/\tau_s)$ , where  $I_{\max}$  is the maximum peak  $\text{Na}^+$  current,  $A_{\infty}$  is a constant value,  $A_f$  and  $A_s$  are fractions of fast and slow inactivating components, and  $\tau_f$  and  $\tau_s$  are the time constants of fast and slow inactivating components, respectively. Results are presented as means  $\pm$  S.E. and statistical comparisons were made using student's  $t$  test. Statistical significance was assumed for  $p < 0.05$ .

All the chemicals were purchased from Sigma (St. Louis, MO) or Wako (Tokyo, Japan) except for mexiletine (gift from Boehringer Ingelheim GmbH, Ingelheim, Germany) and QX-314 (Alomone Labs, Jerusalem, Israel).

## Results

**Enhanced Tonic Block and Attenuated Use-Dependent Block by Mexiletine.** The most remarkable biophysical characteristic of the S1710L channel is the enhancement in closed-state inactivation, fast inactivation, and slow inactivation (Shirai et al., 2002). Because of the enhanced closed-state inactivation, the S1710L channel shows a large negative shift in steady-state inactivation ( $V_{1/2}$ : WT,  $-86.8 \pm 1.1$  mV,  $n = 6$ ; S1710L,  $-108.2 \pm 2.0$  mV,  $n = 5$ ;  $p < 0.001$ ) (Fig. 1B). Consistent with these gating properties, S1710L channels showed mexiletine tonic block ( $300 \mu\text{M}$ ) greater than WT at a holding potential of  $-120$  mV (percentage block: WT,  $64.7 \pm 3.8\%$ ,  $n = 7$ ; S1710L,  $76.8 \pm 2.9\%$ ,  $n = 7$ ;  $p < 0.05$ ). The  $\text{IC}_{50}$  values for mexiletine tonic block in WT and S1710L were 206 and  $159 \mu\text{M}$ , respectively (Fig. 2A). If the tonic block roughly parallels the drug-free voltage-dependence of channel availability, the difference between WT and S1710L should be attenuated when cells are depolarized from very negative holding potential. At a holding potential of  $-150$  mV, the magnitude of mexiletine tonic block ( $300 \mu\text{M}$ ) was diminished for both WT ( $25.7 \pm 2.7\%$ ,  $n = 5$ ) and S1710L ( $53.8 \pm 4.5\%$ ,  $n = 5$ ,  $p < 0.001$ ), but the tonic block at  $-150$

mV was still greater in S1710L ( $\text{IC}_{50}$ : WT,  $542 \mu\text{M}$ ; S1710L,  $273 \mu\text{M}$ ) (Fig. 2B) as it was at  $-120$  mV. These results argue the hypothesis that the enhanced tonic block of the S1710L could be explained simply by an enhanced inactivation of the mutant channel (state-dependent mechanisms); instead, they suggest that some additional mechanisms involving the pore structure may contribute to the modification of the drug access paths, which in turn alters drug affinity.

We next investigated the use-dependent block of mexiletine. In the presence of  $50 \mu\text{M}$  mexiletine, cells were depolarized by 2-Hz train pulses at  $-20$  mV for 400 ms from a holding potential of  $-120$  mV. Because the slow inactivation is enhanced and the recovery from inactivation is delayed in S1710L channels (Akai et al., 2000; Shirai et al., 2002), it is expected that the larger fraction of the channels are inactivated by this protocol, thereby enhancing the use-dependent block in S1710L. Contrary to this assumption, S1710L channels showed a remarkable attenuation in use-dependent block (Fig. 3A). Block ratio at the 30th train pulse over the control  $\text{Na}^+$  current levels for WT and S1710L were  $86.5 \pm 1.2\%$  ( $n = 7$ ) and  $72.7 \pm 1.6\%$  ( $n = 10$ ) ( $p < 0.001$ ), respectively. Diminished use-dependent block in S1710L was also evident under a train pulse protocol with shorter test pulse (20 ms,  $-20$  mV, 8.33 Hz) with the same interpulse duration at 2 Hz (100 ms at  $-120$  mV) (Fig. 3B), suggesting that the contribution of slow inactivation caused by prolonged depolarization to the diminished use-dependent block is negligible if any.

Because the use-dependent block is attained by a balance between the time course of block (during depolarization) and the recovery from block (during repolarization), attenuated mexiletine use-dependent block in S1710L is most probably caused by the accelerated recovery from drug block. To test this hypothesis, recovery for mexiletine block was assessed by using a standard double-pulse protocol in the presence or absence of  $50 \mu\text{M}$  mexiletine (Fig. 3C). Recovery from inactivation without drugs was slower in S1710L; however, recovery from mexiletine block was significantly faster in S1710L than in WT (time to 50% recovery: WT,  $601 \pm 22$  ms,  $n = 4$ ; S1710L,  $181 \pm 7$  ms,  $n = 6$ ;  $p < 0.001$ ). These results suggest that the molecular mechanisms underlying the reduced mexiletine use-dependent block in S1710L include facilitated repriming of channels from mexiletine block, an alternative drug access path created by the mutation at the  $\text{Na}^+$  channel pore, or both.

Open channel blocking properties of mexiletine have been implicated in several  $\text{Na}^+$  channelopathies with inactivation-deficient mutations including type 3 congenital long QT syndrome and paramyotonia congenita (Wang et al., 1997, 2004). It preferentially blocks persistent late  $\text{Na}^+$  current in such diseases states; however, mexiletine preferentially blocks inactivated channels (Kodama et al., 1986) of wild-type and mutant channels without observable late  $\text{Na}^+$  current. Therefore, it is possible to speculate that the diminished use-dependent block is attributable to the reduced mexiletine affinity to the inactivated channels. Steady-state channel availability was determined in the presence or absence of  $100 \mu\text{M}$  mexiletine by using 10-s prepulses ranging from  $-150$  to  $-70$  mV to ensure steady-state before the test pulse (Fig. 3D). Apparent dissociation constant for the inactivated state ( $K_i$ ) was calculated by the Bean's equation (Bean et al., 1983).  $K_i$  for mexiletine was approximately 4-fold greater in S1710L

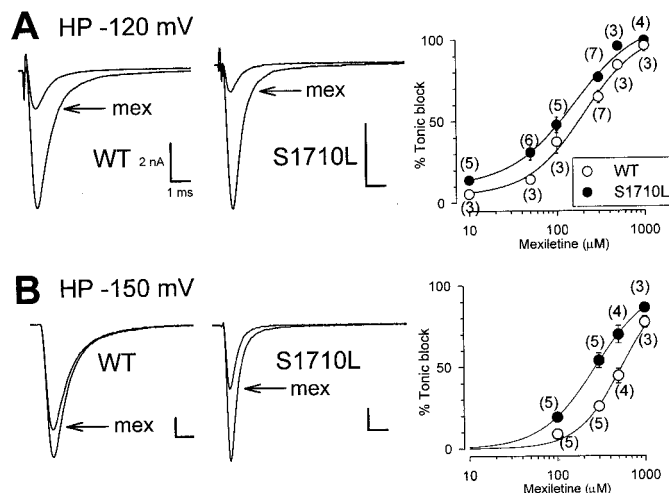


**Fig. 2.** Tonic block by mexiletine. Representative current traces of WT (left) and S1710L (middle) recorded in presence and absence of  $300 \mu\text{M}$  mexiletine (mex). Currents were elicited by a test pulse of  $-20$  mV from a holding potential of  $-120$  mV (A) or  $-150$  mV (B). Currents are normalized by the peak current before mexiletine application and superimposed. Calibrations indicate 2 nA and 1 ms. Concentration-response curves for mexiletine are shown on the right. Normalized peak current was fit with Hill equation:  $B (\%) = 100 / (1 + (D/\text{IC}_{50})^{n_H})$ , where  $B$  is the percentage block at a drug concentration  $D$ , and  $n_H$  is the Hill coefficient. Numbers of the cells analyzed are shown in brackets. The  $\text{IC}_{50}$  values are WT,  $162 \mu\text{M}$ ; S1710L,  $95 \mu\text{M}$  (holding potential,  $-120$  mV), and WT,  $542 \mu\text{M}$ ; S1710L,  $273 \mu\text{M}$  (holding potential,  $-150$  mV).



(WT,  $3.4 \pm 0.9 \mu\text{M}$ ,  $n = 7$ ; S1710L,  $13.8 \pm 1.5 \mu\text{M}$ ,  $n = 8$ ;  $p < 0.001$ ). These results suggest that the affinity to the inactivated channels is significantly reduced in S1710L, despite the fact that S1710L has propensity to enter inactivated

state. These results again disagree with the assumption that the altered pharmacology to Na<sup>+</sup> channel blockers of the mutant Na<sup>+</sup> channel may be explained simply by the state-dependent mechanism (altered gating properties of the mutant channel) and suggest rather that the structural changes at the channel pore per se modify the drug access path.

**Modified Access Paths for Na<sup>+</sup> Channel Blockers Revealed by QX-314.** Most commonly used local anesthetic and antiarrhythmic drugs reach their receptor site located at the inner mouth pore through either the hydrophilic (channel pore) path or hydrophobic path (membrane) (Hille, 1977). A membrane-impermeant quaternary amine QX-314 blocks cardiac Na<sup>+</sup> channel from the outside by passing through the pore (Alpert et al., 1989; Qu et al., 1995), but not Na<sup>+</sup> channel isoforms of brain and skeletal muscle. QX-314 is therefore a useful molecular tool to assess whether the diminished use-dependent block in S1710L channels is caused by the facilitated drug escape through the altered access paths. Extracellularly applied 100  $\mu\text{M}$  QX-314 elicited significantly greater tonic block in S1710L (WT,  $4.1 \pm 1.8\%$ ,  $n = 5$ ; S1710L,  $19.6 \pm 4.1\%$ ,  $n = 8$ ;  $p < 0.05$ ) (Fig. 4, A and B), consistent with the enhanced mexiletine tonic block in S1710L (Fig. 2). If the mutation at the selectivity filter region allows access to the internal binding site, it may also provide an alternative path for dissociation of the bound drug. To determine whether the dissociation through the hydrophilic path is facilitated in S1710L, 100  $\mu\text{M}$  QX-314 was included in the pipette and applied intracellularly, allowing QX-314 diffuse into cell. Five minutes after rupturing the membrane, cells were depolarized by 30 train pulses (2 Hz, 5 ms,  $-20$  mV) to ensure the steady-state use-dependent block, followed by repolarization at  $-150$  mV for a variable length of recovery time to monitor the recovery from QX-314 block. WT

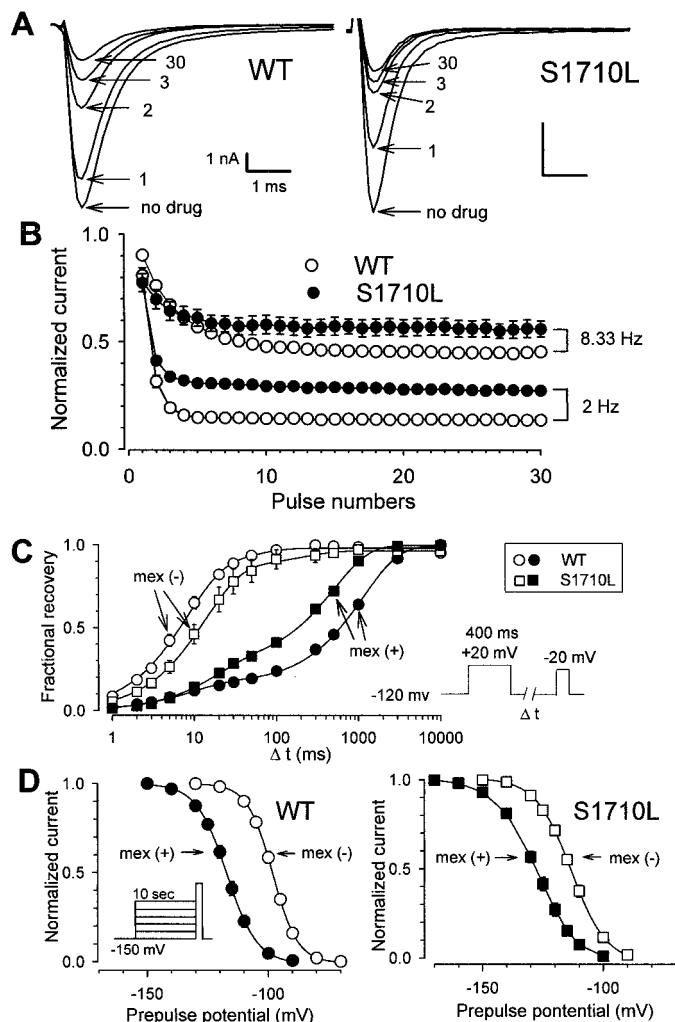


**Fig. 3.** Mexiletine use-dependent block and recovery from block. **A**, a train of 30 repetitive pulses (400 ms,  $-20$  mV) was applied at 2 Hz from a holding potential of  $-120$  mV to produce use-dependent block in the absence or presence of 50  $\mu\text{M}$  mexiletine. Currents are normalized by the peak current before mexiletine application. The numbers indicate 1st (1), 2nd (2), 3rd (3), and 30th (30) of the 2 Hz train. **B**, mexiletine use-dependent block was assessed by applying either train pulses of protocol A (400 ms,  $-20$  mV, 2 Hz) or protocol B (20 ms,  $-20$  mV, 8.33 Hz) after mexiletine perfusion (50  $\mu\text{M}$ ). Interpulse duration between each test pulse was set to 100 ms for both protocols to maintain the recovery time. **C**, time course of recovery from inactivation was assessed by the standard double-pulse protocol shown in the inset in the presence or absence of 50  $\mu\text{M}$  mexiletine (mex). Fractional recovery was determined as the ratio of peak currents measured at  $-20$  mV after a given test interval to the maximum peak current, and fit with double exponential function. **D**, dissociation constant for inactivated channels. Cells were depolarized by prepulses ranging from  $-150$  to  $-70$  mV for 10 s from a holding potential of  $-150$  mV to ensure the steady-state inactivation, followed by a test pulse at  $-20$  mV in the presence or absence of 100  $\mu\text{M}$  mexiletine (mex). Peak Na<sup>+</sup> currents were normalized to the maximum Na<sup>+</sup> current and data were fit with a Boltzmann equation. Dissociation constant for the inactivated state ( $K_i$ ) was calculated according to the Bean's equation (Bean et al., 1983):  $V_{1/2} - V_{1/2c} = k \times \ln((1 + D/K_i)/(1 + D/K_r))$ , where  $V_{1/2}$  and  $V_{1/2c}$  are the midpoints of steady-state inactivation for mexiletine (100  $\mu\text{M}$ ) and control, respectively,  $D$  is the mexiletine concentration, and  $K_r$  is the dissociation constant for the resting state. The  $K_r$  values are equivalent to the  $\text{IC}_{50}$  values measured with a holding potential of  $-150$  mV (WT, 542  $\mu\text{M}$ ; S1710L, 273  $\mu\text{M}$ ; Fig. 2B).

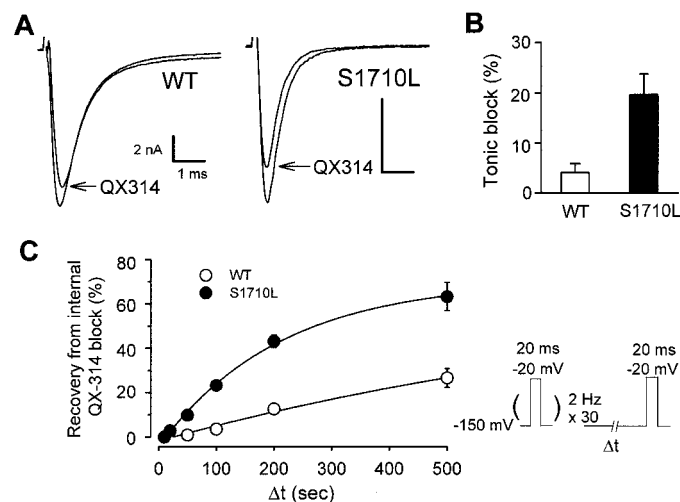


**Fig. 4.** Tonic block and recovery from use-dependent block by QX-314. **A** and **B**, representative current traces in the presence or absence of an externally applied 100  $\mu\text{M}$  QX-314. Cells were depolarized at  $-20$  mV from the holding potential of  $-150$  mV. Externally applied QX-314 elicited minimal tonic block in WT, whereas S1710L showed significantly enhanced tonic block. **C**, time course of recovery from block by internally applied 100  $\mu\text{M}$  QX-314. Recovery from block was assessed by a pulse protocol as shown in the inset. Currents were normalized by the difference between the peak current elicited by the 1st pulse and 30th pulses. Peak currents during recovery were normalized by the difference between the peak current during the first pulse of a train and the 10-s recovery test pulse, and plotted as recovery: Recovery % =  $(I - I_{30th})/(I_{1st} - I_{30th}) \times 100$ . Data were fit with the single exponential equation.

channel recovered from internal QX-314 block very slowly with a time constant ( $\tau$ ) of  $905 \pm 212$  s ( $n = 6$ ), whereas the S1710L channel recovered 4.3-fold faster than WT ( $\tau = 207 \pm 23$  s,  $n = 10$ ,  $p < 0.001$ ; Fig. 4C). These results suggest that the structural changes at the pore region in the S1710L channel alter the escape path of the antiarrhythmic drugs from the inner drug binding site.

**Permeation Properties of S1710L.** Mutations at the putative selectivity filter residues change ion permeation properties of  $\text{Na}^+$  channels (Chiamvimonvat et al., 1996; Favre et al., 1996; Tsushima et al., 1997). Moreover, the selectivity filter also regulates antiarrhythmic drug binding (Sunami et al., 1997). However, it remains unclear whether the residue Ser1710, next to the selectivity filter residue in domain 4, is buried in the membrane or faces the hydrophilic ion-conducting pore. To elucidate the molecular location of this residue within the  $\text{Na}^+$  channel pore, we tested the permeation properties and ion selectivity in S1710L channel. When current-voltage relationship was measured using the standard  $\text{Cs}^+/\text{Na}^+$  pipette solution, the reversal potential was comparable between WT and S1710L (Fig. 5A). However, when measured with the  $\text{K}^+/\text{Na}^+$  pipette solution, the reversal potential of S1710L was significantly shifted in the hyperpolarizing direction (WT,  $43.5 \pm 0.79$  mV,  $n = 5$ ; S1710L,  $36.8 \pm 0.40$  mV,  $n = 6$ ;  $p < 0.001$ ; Fig. 5B), and the peak potential was shifted in the depolarizing direction. These results suggest that the ion selectivity of the S1710L channel was altered.

To analyze the ion selectivity more quantitatively, currents were recorded using standard bath or with a high  $\text{K}^+$  solution in which  $\text{Na}^+$  was replaced with equimolar  $\text{K}^+$ . Figure 5, C and D, shows the representative current traces of WT (C) and S1710L (D) in the presence of two different bath solutions and the corresponding current-voltage relationship. Although the ratios of the peak currents measured in two different bath solutions were comparable between WT and S1710L, the reversal potential measured of S1710L was significantly shifted toward depolarizing direction (WT,  $5.6 \pm 1.7$  mV,  $n = 5$ ; S1710L,  $20.8 \pm 2.7$  mV,  $n = 4$ ;  $p < 0.005$ ). The calculated  $\text{K}^+$  permeability ( $P_{\text{K}}/P_{\text{Na}}$ ) was 1.9-fold higher in S1710L than WT (WT,  $0.091 \pm 0.005$ ,  $n = 5$ ; S1710L,  $0.169 \pm 0.017$ ,  $n = 4$ ;  $p < 0.005$ ), indicating ion selectivity defect in the S1710L channel. One possible explanation for these observations is that the residue Ser1710 next to the D4 filter residue Ala1711 faces the hydrophilic ion-conducting pore, and the mutation of this residue results in functional changes in both antiarrhythmic drug affinity and ion selectivity.

## Discussion

Gating properties of  $\text{Na}^+$  channels are the primary determinants of pharmacological and clinical efficacy of  $\text{Na}^+$  channel blockers. In the present study, we found that the selectivity filter region is the structural determinant of the actions of these drugs using a cardiac  $\text{Na}^+$  channel pore mutation associated with idiopathic ventricular fibrillation (Akai et al., 2000; Shirai et al., 2002). The mutant channel showed augmented mexiletine tonic block and a paradoxically attenuated use-dependent block. These pharmacological characteristics are attributable to the structural changes at the selectivity filter region rather than the secondary changes in

state-dependent  $\text{Na}^+$  channel blocker sensitivity because of gating modulations. The present study further supports the previous observations by Sunami et al. (1997) and Huang et al. (2000) that residues at the  $\text{Na}^+$  channel selectivity filter region are the crucial determinants for the pharmacological responses to  $\text{Na}^+$  channel blockers as well as for ion selectivity.

The aromatic residues Phe1760 and Tyr1767 (Fig. 6A, F and Y) on D4/S6 comprise a part of the crucial binding site for local anesthetics and class I antiarrhythmic drugs (Ragsdale

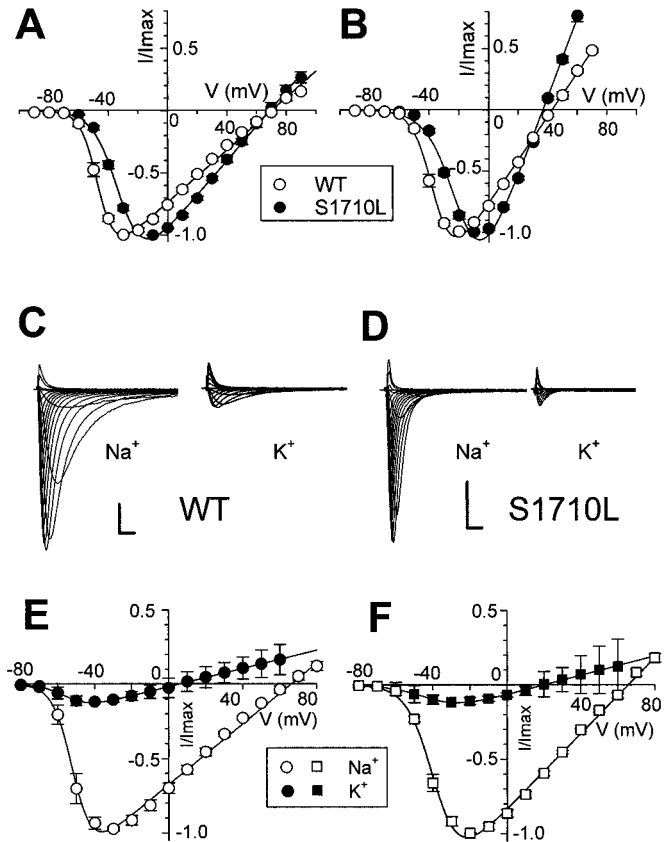


**Fig. 5.** Permeation properties of WT and S1710L channels. A and B, current-voltage relationship of WT and S1710L channels measured by using standard  $\text{Cs}^+/\text{Na}^+$  pipette solution (A) or  $\text{K}^+/\text{Na}^+$  pipette solution (B) (see *Material and Methods* for details). Data were fit with the Boltzmann distribution:  $I = (V - V_r) \times G_{\text{max}} \times (1 + \exp((V - V_{1/2})/k))^{-1}$ , where  $I$  is the peak  $\text{Na}^+$  current,  $V_r$  is the reversal potential,  $G_{\text{max}}$  is the maximal slope conductance,  $V_{1/2}$  is the mid point of the activation, and  $k$  is the slope factor. Reversal potential of S1710L was comparable with WT when recorded with the standard  $\text{Cs}^+/\text{Na}^+$  pipette solution (A), but it was significantly shifted in the negative direction with more physiological pipette solution (B). C and D, to test the permeability to  $\text{Na}^+$  and  $\text{K}^+$ , whole-cell current was measured with the standard bath solution containing 145 mM NaCl or a modified buffer in which 145 mM NaCl was replaced by equimolar KCl.  $\text{Cs}^+/\text{Na}^+$  solution was applied in the pipettes. Representative current traces recorded from WT (C) or S1710L (D) using either standard bath solution or  $\text{K}^+$ -rich solution. Calibration bars indicate 2 nA and 1 ms. E and F, peak current-voltage relationships of WT (E) and S1710L (F) using either standard bath solution (open symbols) and  $\text{K}^+$  rich solution (closed symbols). The current scale is normalized to the standard solution. Peak current-voltage relationship was fit with the Boltzmann distribution. Permeability ratio for  $\text{Na}^+$  and  $\text{K}^+$  ( $P_{\text{K}}/P_{\text{Na}}$ ) was calculated using the a modified Goldman-Hodgkin-Katz equation:  $P_{\text{K}}/P_{\text{Na}} = ([\text{Na}]_o/[\text{K}]_o) \times \exp((E_{\text{K}} - E_{\text{Na}}) \times F/RT)$ , where  $E_{\text{K}}$  and  $E_{\text{Na}}$  are the reversal potentials for the  $\text{K}^+$  and  $\text{Na}^+$ , respectively,  $R$  is the gas constant,  $T$  is absolute temperature, and  $F$  is the Faraday constant (Sun et al., 1997; Hille, 2001). Current ratios were calculated from peak inward currents in the presence of  $\text{K}^+$  normalized to the peak current in  $\text{Na}^+$  solution.

et al., 1994; Ragsdale et al., 1996). In addition to these residues, biophysical evidence has shown that the selectivity filter residues of four P-loops (Asp372, Glu898, Lys1419, Ala1711) (Sunami et al., 1997), and Ile1756 (Ragsdale et al., 1994; Sunami et al., 2001) affect local anesthetic drug binding and modify its access pathway. Moreover, isoform-specific differences in extracellularly applied QX-314 or QX-222 block have been attributed to the cardiac-specific residues Thr1753 near the extracellular end of D4/S6 (Fig. 6A, T) (Qu et al., 1995) and Cys373 (Fig. 6A, C) next to the D1 selectivity filter residue (Sunami et al., 2000). These data support the notion that D4/S6, all four selectivity filter residues, and one neighboring residue in the D1 P-loop are spatially near each other and may constitute structure responsible for binding and access of Na<sup>+</sup> channel blockers. Our study provides further evidence that residues near the D4 selectivity filter are involved in ion selectivity as well as the access and the dissociation of Na<sup>+</sup> channel blockers.

The ion selectivity of the Na<sup>+</sup> channel is determined by a ring of amino acids created by the P-loops of all four domains (D1–D4), and the major determinants are the residues referred to as 'DEKA' (Asp372, Glu898, Lys1419, and Ala1711; following residue numbers are the equivalents of human Na<sub>v</sub>1.5) (Heinemann et al., 1992; Sun et al., 1997) (Fig. 6A). However, the contribution of each P-loop to the ion selectivity is not equal (Schlief et al., 1996). Site-directed mutagenesis studies have shown that the positive Lys residue in D3 is the most critical residue for ion selectivity (Chiamvimonvat et al., 1996). In contrast, the physiological role of the D4 selectivity filter region is less clear. Cysteine mutagenesis experiments have shown that the five residues between Ser1710 and Asp1714 around the selectivity filter residue Ala1711 are all accessible from outside (Chiamvimonvat et al., 1996), suggesting that these five residues face the hydrophilic ion-

conducting pore. In fact, mutations at the residues carboxy-terminal to the Ala1711 (Glu1712, Trp1713, Asp1714) change the ion selectivity (Chiamvimonvat et al., 1996; Tsushima et al., 1997) (Fig. 6B). Our observations further support the idea that the Ser1710 located at amino-terminal next to the D4 selectivity filter residue probably faces the ion-conducting pore and contributes to the ion selectivity. However, we cannot exclude the possibility that the amino acid change at the Ser1710 may result in an indirect alteration of the tertiary structure required for permeation properties rather than a direct change at the hydrophilic ion conduction pore. More detailed studies using site-directed mutagenesis are required to elucidate the underlying mechanisms.

The molecular mechanism by which QX-314 accesses the internal binding site is not simple. Because rate of the block by extracellular application QX-314 is reduced by an extracellularly acting pore blocker tetrodotoxin, QX-314 moves through the pore in reaching its receptor site (Qu et al., 1995). However, the diameter of the QX-314 molecule is larger than the cut-off area of Na<sup>+</sup> channel ( $3.2 \times 5.2$  Å), so it is not likely that the molecule accesses the binding site from outside and exits from it directly through the aqueous pore by diffusion; instead, it is conceivable that the charged aliphatic portion of the drug may use the direct route through the pore through the selectivity filter while the rest of the molecule slips out the through interface between P-loop and S6 helices (Lee et al., 2001). Furthermore, because the mutation at the D3 selectivity filter residue permeates molecules of diameter severalfold larger than the Na<sup>+</sup> channel pore (Huang et al., 2000), it is possible that hydrophobic interfaces contiguous to the D4 selectivity filter residue may also facilitate the permeation of larger molecules. On the other hand, the mutation at the selectivity filter region may structurally change the interfaces between D4 P-loop and

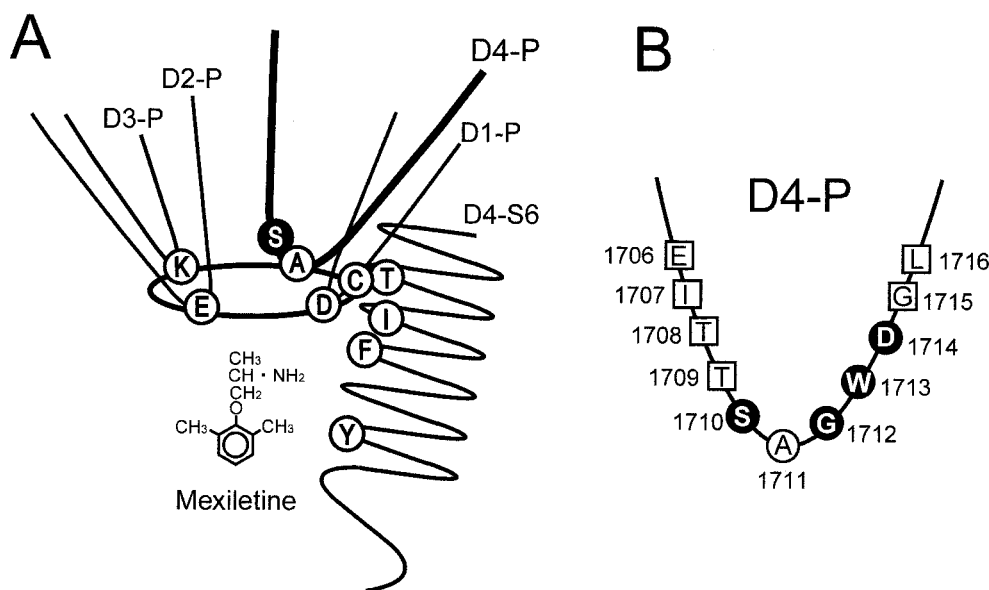


**Fig. 6.** Schematic representation of the cardiac Na<sup>+</sup> channel pore structure. A, side view of the Na<sup>+</sup> channel pore composed of four P-loops and the D4/S6. Closed circles Phe1760 and Tyr1767 represent local anesthetic/antiarrhythmic binding site. Selectivity filter residues DEKA motif (Sunami et al., 1997) (Asp372, Glu898, Lys1419, Ala1711; shown as an oval) and the Ile1756 (Ragsdale et al., 1994; Sunami et al., 2001) on D4/S6 affect drug binding and access pathway. Cardiac specific residues Thr1753 (Qu et al., 1995) on the extracellular end of D4/S6 and Cys373 (Sunami et al., 2000) next to the D1 selectivity filter residue are responsible for the access to the binding site of extracellularly applied QX-314 or QX-222. Ser1710 (this study) affect both ion permeation and drug access. B, amino acid sequence of D4-S6. Five residues Thr1710–Asp1714 around the selectivity filter residue Ala1711 are all accessible from outside (Chiamvimonvat et al., 1996) (circles). Glu1712, Trp1713, Asp1714 (Chiamvimonvat et al., 1996; Tsushima et al., 1997), and Ser1710 (this study) affect the ion selectivity (●).



other transmembrane helices, which in turn creates crevices in the hydrophobic core of protein and facilitates the access and egress of mexiletine and QX-314. It is plausible to speculate that a ridge involving residues located at both descending and ascending limbs of the D4 P-loop, rather than a discrete ring composed of the four residues creating constriction in the pore, may contribute to the Na<sup>+</sup> channel selectivity (Fig. 6B).

Brugada syndrome is a subtype of idiopathic ventricular fibrillation characterized by electrocardiographic findings of ST elevation in the right precordial leads. Molecular basis of Brugada syndrome are various functional defects in cardiac Na<sup>+</sup> channel gating, most of which result in reduction of Na<sup>+</sup> current density (loss of function) (Keating and Sanguinetti, 2001). Na<sup>+</sup> channel blockers are clinically used as diagnostic tools for Brugada syndrome to provoke or unmask ST elevation (Brugada et al., 2000). A plausible explanation for the proarrhythmic sensitivity to Na<sup>+</sup> channel blockers is the enhanced closed-state inactivation and the inactivation intermediate between fast and slow inactivation (I<sub>M</sub>) recently demonstrated in an cardiac Na<sup>+</sup> channel mutation 1795insD (Viswanathan et al., 2001). It is evident that large negative shift of steady-state inactivation (Fig. 1B) and enhanced closed-state inactivation and slow inactivation in the S1710L channel (Shirai et al., 2002) are consistent with the enhanced mexiletine tonic block (Fig. 2) and QX-314 tonic block (Fig. 4, A and B). However, such gating changes do not accommodate the paradoxical attenuation of mexiletine use-dependent block (Fig. 3, A and B), reduced mexiletine affinity for the inactivated state (K<sub>i</sub>; Fig. 3D), or accelerated recovery from mexiletine and QX-314 block (Figs. 3C and 4C). Lee et al. (2001) have shown that accelerated recovery from use-dependent block was previously identified in the cardiac isoform specific mutations D1 P-loop and D4/S6, and these residues define the cardiac-specific external paths for the Na channel blockers. It is speculated that the S1710L mutation at the D4 P-loop may change the selectivity filter region and impair the restriction of drug access to and egress from the internal binding site, and inefficient trapping of the drug within the vestibule results in attenuating the use-dependent block. It is obvious that electrocardiographic manifestations in response to Na<sup>+</sup> channel blockers are intriguing from both clinical and pharmacological standpoints; however, the drug provocation test has not been performed because the patient has already received an implantable cardioverter defibrillator and refuses the drug test.

In summary, our results suggest that the substitution of Ser1710 next to the putative selectivity filter residue of the D4 results in structural alterations of the external path of the Na<sup>+</sup> channel pore toward drug binding site. Facilitated drug escape through the external path because of the SCN5A mutation may be responsible, at least in part, for clinical and pharmacological manifestations of cardiac Na<sup>+</sup> channelopathies, depending upon the location of the mutations.

#### Acknowledgments

We are indebted to Drs. A. L. George and J. R. Balser for helpful discussion. The technical assistance of A. Aita and K. Morisaki is also appreciated.

#### References

Akai J, Makita N, Sakurada H, Shirai N, Ueda K, Kitabatake A, Nakazawa K, Kimura A, and Hiraoka M (2000) A novel SCN5A mutation associated with

- idiopathic ventricular fibrillation without typical ECG findings of Brugada syndrome. *FEBS Lett* **479**:29–34.
- Alpert LA, Fozzard HA, Hanck DA, and Makielski JC (1989) Is there a second external lidocaine binding site on mammalian cardiac cells? *Am J Physiol* **257**: H79–H84.
- Bean B, Cohen C, and Tsien R (1983) Lidocaine block of cardiac sodium channels. *J Gen Physiol* **81**:613–642.
- Brugada R, Brugada J, Antzelevitch C, Kirsch GE, Potenza D, Towbin JA, and Brugada P (2000) Sodium channel blockers identify risk for sudden death in patients with ST-segment elevation and right bundle branch block but structurally normal hearts. *Circulation* **101**:510–515.
- Catterall WA (2000) From ionic currents to molecular mechanisms: the structure and function of voltage-gated sodium channels. *Neuron* **26**:13–25.
- Chiamvimonvat N, Perez-Garcia MT, Ranjan R, Marban E, and Tomaselli GF (1996) Depth asymmetries of the pore-lining segments of the Na<sup>+</sup> channel revealed by cysteine mutagenesis. *Neuron* **16**:1037–1047.
- Favre I, Moczydlowski E, and Schild L (1996) On the structural basis for ionic selectivity among Na<sup>+</sup>, K<sup>+</sup> and Ca<sup>2+</sup> in the voltage-gated sodium channel. *Biophys J* **71**:3110–3125.
- Heinemann SH, Terlau H, Stuhmer W, Imoto K, and Numa S (1992) Calcium channel characteristics conferred on the sodium channel by single mutations. *Nature (Lond)* **356**:441–443.
- Hille B (1977) Local anesthetics: hydrophilic and hydrophobic pathways for the drug-receptor reaction. *J Gen Physiol* **69**:497–515.
- Hille B (2001) *Ion Channels of Excitable Membranes*. 3rd ed. Sinauer Associates, Inc., Sunderland, MA.
- Hondeghem LM and Katzung BG (1977) Time- and voltage-dependent interactions of antiarrhythmic drugs with cardiac sodium channels. *Biochim Biophys Acta* **472**: 373–398.
- Huang CJ, Favre I, and Moczydlowski E (2000) Permeation of large tetraalkylammonium cations through mutant and wild-type voltage-gated sodium channels as revealed by relief of block at high voltage. *J Gen Physiol* **115**:435–454.
- Keating MT and Sanguinetti MC (2001) Molecular and cellular mechanisms of cardiac arrhythmias. *Cell* **104**:569–580.
- Kodama I, Toyama J, and Yamada K (1986) Open and inactivated sodium channel block by class-I antiarrhythmic drugs. *Jpn Heart J* **27 Suppl 1**:83–89.
- Lee PJ, Sunami A, and Fozzard HA (2001) Cardiac-specific external paths for lidocaine, defined by isoform-specific residues, accelerate recovery from use-dependent block. *Circ Res* **89**:1014–1021.
- Lipkind GM and Fozzard HA (2000) KcsA crystal structure as framework for a molecular model of the Na<sup>+</sup> channel pore. *Biochemistry* **39**:8161–8170.
- Nuss HB, Kambouris NG, Marban E, Tomaselli GF, and Balser JR (2000) Isoform-specific lidocaine block of sodium channels explained by differences in gating. *Biophys J* **78**:200–210.
- Qu Y, Rogers J, Tanada T, Scheuer T, and Catterall WA (1995) Molecular determinants of drug access to the receptor site for antiarrhythmic drugs in the cardiac Na<sup>+</sup> channel. *Proc Natl Acad Sci USA* **92**:11839–43.
- Ragsdale DS, McPhee JC, Scheuer T, and Catterall WA (1994) Molecular determinants of state-dependent block of Na<sup>+</sup> channels by local anesthetics. *Science (Wash DC)* **265**:1724–1728.
- Ragsdale DS, McPhee JC, Scheuer T, and Catterall WA (1996) Common molecular determinants of local anesthetic, antiarrhythmic and anticonvulsant block of voltage-gated Na<sup>+</sup> channels. *Proc Natl Acad Sci USA* **93**:9270–9275.
- Schlieff T, Schonherr R, Imoto K, and Heinemann SH (1996) Pore properties of rat brain II sodium channels mutated in the selectivity filter domain. *Eur Biophys J* **25**:75–91.
- Shirai N, Makita N, Sasaki K, Yokoi H, Sakuma I, Sakurada H, Akai J, Kimura A, Hiraoka M, and Kitabatake A (2002) A mutant cardiac sodium channel with multiple biophysical defects associated with overlapping clinical features of Brugada syndrome and cardiac conduction disease. *Cardiovasc Res* **53**:348–354.
- Sun YM, Favre I, Schild L, and Moczydlowski E (1997) On the structural basis for size-selective permeation of organic cations through the voltage-gated sodium channel. Effect of alanine mutations at the DEKA locus on selectivity, inhibition by Ca<sup>2+</sup> and H<sup>+</sup> and molecular sieving. *J Gen Physiol* **110**:693–715.
- Sunami A, Dudley SC Jr, and Fozzard HA (1997) Sodium channel selectivity filter regulates antiarrhythmic drug binding. *Proc Natl Acad Sci USA* **94**:14126–31.
- Sunami A, Glaaser IW, and Fozzard HA (2000) A critical residue for isoform difference in tetrodotoxin affinity is a molecular determinant of the external access path for local anesthetics in the cardiac sodium channel. *Proc Natl Acad Sci USA* **97**:2326–2331.
- Sunami A, Glaaser IW, and Fozzard HA (2001) Structural and gating changes of the sodium channel induced by mutation of a residue in the upper third of IVS6, creating an external access path for local anesthetics. *Mol Pharmacol* **59**:684–691.
- Tsushima RG, Li RA, and Backx PH (1997) Altered ionic selectivity of the sodium channel revealed by cysteine mutations within the pore. *J Gen Physiol* **109**:463–475.
- Viswanathan PC, Bezzina CR, George AL Jr, Roden DM, Wilde AA, and Balser JR (2001) Gating-dependent mechanisms for flecainide action in SCN5A-linked arrhythmia syndromes. *Circulation* **104**:1200–1205.
- Wang DW, Yazawa K, Makita N, George AL Jr, and Bennett PB (1997) Pharmacological targeting of long QT mutant sodium channels. *J Clin Invest* **99**:1714–1720.
- Wang GK, Russell C, and Wang SY (2004) Mexiletine block of wild-type and inactivation-deficient human skeletal muscle hNav1.4 Na<sup>+</sup> channels. *J Physiol* **554**: 621–633.

**Address correspondence to:** Dr. Naomasa Makita, Department of Cardiovascular Medicine, Hokkaido University Graduate School of Medicine, Kita-15, Nishi-7, Kita-Ku, Sapporo, 060-8638, Japan. E-mail: makitan@med.hokudai.ac.jp